

]

Isotope effect on the electron band structure of doped insulators

P.E. Kornilovitch ¹ and A.S. Alexandrov²

¹*Hewlett-Packard, MS 321A, 1000 NE Circle blvd,
Corvallis, Oregon 97330, USA*

²*Department of Physics, Loughborough University,
Loughborough LE11 3TU, UK*

Applying a continuous-time quantum Monte-Carlo algorithm we calculate the exact coherent band dispersion and the density of states of a two dimensional lattice polaron in the region of parameters where any approximation might fail. We find an isotope effect on the band structure, which is different for different wave-vectors of the Brillouin zone and depends on the radius and strength of the electron-phonon interaction. An isotope effect on the electron spectral function is also discussed.

PACS numbers: PACS: 74.72.-h, 74.20.Mn, 74.20.Rp, 74.25.Dw

The isotope substitution, where an ion mass M is varied without any change of electronic configurations, is a powerful tool in testing the origin of electron correlations in solids. In particular, a finite value of the isotope exponent $\alpha = -d \ln T_c / d \ln M$ [1] proved that the superconducting phase transition at $T = T_c$ is driven by the electron-phonon (e-ph) interaction in conventional low-temperature superconductors. Advances in the fabrication of isotope substituted samples made it possible to measure a sizable isotope effect also in many high-temperature superconductors. This led to a general conclusion that phonons are relevant for high T_c . Essential features of the isotope effect on T_c , in particular its large values in low T_c cuprates, an overall trend to decrease as T_c increases, and a small or even negative α in some high T_c cuprates, could be understood in the framework of the bipolaron theory of high-temperature superconductivity [2].

The most compelling evidence for (bi)polaronic carries in novel superconductors was provided by the discovery of a substantial isotope effect on the (super)carrier mass [3, 4]. The effect was observed by measuring the magnetic field penetration depth λ_H of isotope-substituted copper oxides. The carrier density is unchanged with the isotope substitution of O^{16} by O^{18} , so that the isotope effect on λ_H measures directly the isotope effect on the carrier mass m^* . A carrier mass isotope exponent $\alpha_m = d \ln m^* / d \ln M$ was observed, as predicted by the bipolaron theory [2]. In ordinary metals, where the Migdal adiabatic approximation is believed to be valid, $\alpha_m = 0$ is expected. However, when the e-ph interaction is sufficiently strong and electrons form polarons (quasi-particles dressed by lattice distortions), their effective mass m^* depends on M as $m^* = m \exp(\gamma E_p / \omega)$. Here m is the band mass in the absence of the electron-phonon interaction, E_p is the polaron binding energy (polaron level shift), γ is a numerical constant less than 1 that depends on the radius of the electron-phonon interaction, and ω is a characteristic phonon frequency (we use $\hbar = 1$). In the expression for m^* , only the phonon fre-

quency depends on the ion mass. Thus there is a large isotope effect on the carrier mass in (bi)polaronic conductors, $\alpha_m = (1/2) \ln(m^*/m)$ [2], in contrast with the zero isotope effect in ordinary metals.

Recent high resolution angle resolved photoemission spectroscopy (ARPES) [6] provided another compelling evidence for a strong e-ph interaction in the cuprates. It revealed a fine phonon structure in the electron self-energy of the underdoped $La_{2-x}Sr_xCuO_4$ samples [7], and a complicated isotope effect on the electron spectral function in $Bi2212$ [8]. Polaronic carriers were also observed in colossal magneto-resistance manganites including their low-temperature ferromagnetic phase, where an isotope effect on the residual resistivity was measured and explained [9].

These and many other experimental and theoretical observations point towards unusual e-ph interactions in complex oxides, which remain to be quantitatively addressed. While the many-particle e-ph problem has been solved in the weak-coupling, $\lambda \equiv E_p / zt \ll 1$ [5, 10, 11], and in the strong-coupling $\lambda \gg 1$ [12] limits, any analytical or even semi-analytical approximation (i.e. dynamic mean-field approach in finite dimensions) is refutable in the relevant intermediate region of the coupling strength, $\lambda \simeq 1$, and of the adiabatic ratio, $\omega/t \simeq 1$. Here t and z are the nearest neighbor hopping integral and the coordination number of the rigid lattice, respectively.

Advanced variational [13], direct diagonalization [14], and quantum Monte Carlo (QMC) [15, 16, 17] techniques addressed the problem in the intermediate region of parameters, but mainly in the framework of the Holstein model [18] with a local (short-range) e-ph interaction, or in the continuous (effective mass) approximation for the bare electron band [17]. However, in cuprates there is virtually no screening of c -axis polarised optical phonons because an upper limit for the out-of-plane plasmon frequency ($\lesssim 200 \text{ cm}^{-1}$ [19]) is well below the characteristic phonon frequency $\omega \simeq 1000 \text{ cm}^{-1}$. Hence, the unscreened long-range Fröhlich interaction is important in cuprates and other ionic charge-transfer insulators

[13, 20, 21, 22, 23]. A parameter-free estimate [24] yields $E_p \simeq 1$ eV with this interaction alone, which is larger than a magnetic (i.e. exchange J) interaction almost by one order of magnitude. Qualitatively, a longer-range e-ph interaction results in a lighter mass of dressed carries ($\gamma < 1$) because the extended lattice deformation changes gradually in the process of tunnelling through the lattice [20, 21]. Also in the intermediate and strong-coupling regime the finite bandwidth is important, so that the effective mass approximation cannot be applied.

In this Letter we calculate isotope effects on the whole coherent band-structure and DOS of a two-dimensional lattice polaron with short- and long-range e-ph interactions by applying a continuous-time QMC algorithm. Unlike the strong-coupling limit [2] the isotope effect depends on the wave vector in the intermediate region of parameters. We also discuss the isotope effect on the electron spectral function including its incoherent part.

Our model Hamiltonian describes any-radius e-ph interaction of an electron (or hole) on a square-lattice plane with linearly polarized vibrations of all ions of the 3D crystal [21],

$$H = - \sum_{\mathbf{m}, \mathbf{n}} [t(\mathbf{m} - \mathbf{n}) c_{\mathbf{m}}^\dagger c_{\mathbf{n}} + f(\mathbf{m} - \mathbf{n}) \xi_{\mathbf{n}} c_{\mathbf{m}}^\dagger c_{\mathbf{m}}] + \omega \sum_{\mathbf{q}} b_{\mathbf{q}}^\dagger b_{\mathbf{q}} \quad (1)$$

Here $c_{\mathbf{m}}$, and $b_{\mathbf{q}}$ are annihilation electron and phonon operators, respectively, $t(\mathbf{m} - \mathbf{n})$ is the hopping integral, which is nonzero only for the nearest neighbors, $t(\mathbf{a}) \equiv t$ (\mathbf{a} is the primitive lattice vector), $\xi_{\mathbf{n}} = (2NM\omega)^{-1/2} \sum_{\mathbf{q}} e^{i\mathbf{q} \cdot \mathbf{n}} b_{\mathbf{q}} + H.c.$ is the displacement operator at cite \mathbf{n} , N is the number of cells, and $f(\mathbf{m} - \mathbf{n})$ is a “force” applied to the electron at site \mathbf{m} due to the ion displacement at cite \mathbf{n} .

In the strong-coupling, $\lambda \gg 1$, and non-adiabatic limit $\omega \gtrsim t$ one can apply the Lang-Firsov transformation [25] to obtain the ground state energy $E_p = (2M\omega)^{-2} \sum_{\mathbf{m}} f^2(\mathbf{m})$ and the coherent polaron band dispersion $\epsilon_{\mathbf{k}} = E_{\mathbf{k}} \exp(-g^2)$ with the polaron narrowing exponent $g^2 = (2M\omega^3)^{-1} \sum_{\mathbf{m}} [f^2(\mathbf{m}) - f(\mathbf{m})f(\mathbf{m} + \mathbf{a})]$ and the “bare” band dispersion $E_{\mathbf{k}}$. The band-structure isotope exponent α_b does not depend on the wave-vector \mathbf{k} in this limit, because e-ph interactions do not change the band topology,

$$\alpha_b \equiv -\frac{\partial \ln \epsilon_{\mathbf{k}}}{\partial \ln M} = \frac{g^2}{2}. \quad (2)$$

It is the same as α_m . If the interaction is short-range, $f(\mathbf{m} - \mathbf{n}) \propto \delta_{\mathbf{m}, \mathbf{n}}$ (the Holstein model), then $g^2 = E_p/\omega$. Generally, one has $g^2 = \gamma E_p/\omega$ with the numerical coefficient $\gamma = (1 - \sum_{\mathbf{m}} f(\mathbf{m})f(\mathbf{m} + \mathbf{a})) / \sum_{\mathbf{n}} f^2(\mathbf{n})$. γ can be significantly less than 1 for a long-range (Fröhlich) interaction [20], such as the unscreened interaction with c -axis vibrations of apex oxygen ions in the cuprates [21]:

$$f(\mathbf{m} - \mathbf{n}) \propto (|\mathbf{m} - \mathbf{n}|^2 + 1)^{-3/2}. \quad (3)$$

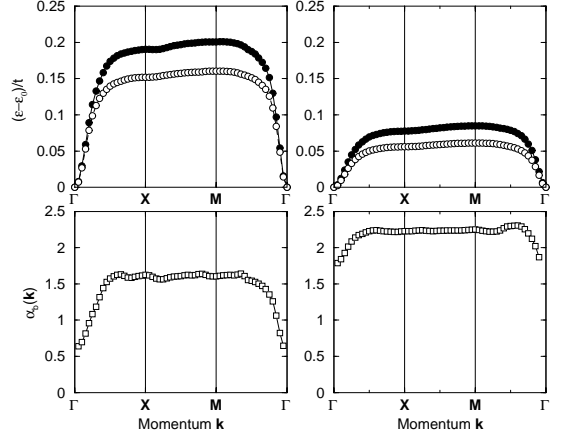


FIG. 1: Top panels: small Holstein polaron band dispersions along the main directions of the two-dimensional Brillouin zone. Left: $\lambda = 1.1$, right: $\lambda = 1.2$. Filled symbols is $\omega = 0.70t$, open symbols is $\omega = 0.66t$. Lower panels: the band structure isotope exponent for $\lambda = 1.1$ (left) and $\lambda = 1.2$ (right).

Here the distance between the in-plane and apex cites $\sqrt{|\mathbf{m} - \mathbf{n}|^2 + 1}$ is measured in units of the in-plane lattice constant a , and the apex-plane distance is taken to be also a . Thus the strong-coupling isotope exponent, Eq. (2) turns out to be numerically smaller for a longer-range e-ph interaction compared with a short-range interaction of the same strength E_p .

QMC results (see below) show that this tendency also holds in the intermediate coupling regime, but the isotope exponent becomes a nontrivial function of the wave vector: $\alpha_b = \alpha_b(\mathbf{k})$, because e-ph interactions substantially modify the band topology in this regime. We apply a continuous-time path-integral QMC algorithm developed by one of us [26], which is free from any systematic finite-size and finite-time-step errors. The finite-temperature errors are exponentially small when the simulation temperature is smaller than the phonon frequency. The method allows for *exact* calculation of the whole polaron band dispersion on any-dimensional infinite lattice with any-range e-ph interaction using the many-body path integral,

$$\epsilon_0 = \frac{\int \mathcal{D}\mathbf{r} \mathcal{D}\xi \cdot w \cdot \left[-\frac{\partial w}{\partial \beta} \right]}{\int \mathcal{D}\mathbf{r} \mathcal{D}\xi \cdot w}, \quad (4)$$

$$\epsilon_{\mathbf{k}} - \epsilon_0 = -\frac{1}{\beta} \ln \left\{ \frac{\int \mathcal{D}\mathbf{r} \mathcal{D}\xi \cdot w \cdot e^{i\mathbf{k} \cdot \Delta\mathbf{r}}}{\int \mathcal{D}\mathbf{r} \mathcal{D}\xi \cdot w} \right\}, \quad (5)$$

where ϵ_0 is the ground state energy. Configurations described by the electron position vector \mathbf{r} and ion displacements ξ , are obtained at imaginary time $\tau = \beta = 1/(k_B T)$ from the configurations at $\tau = 0$ by shifting along the lattice by vectors $\Delta\mathbf{r}$. $\int \mathcal{D}\mathbf{r} \mathcal{D}\xi$ integrates over

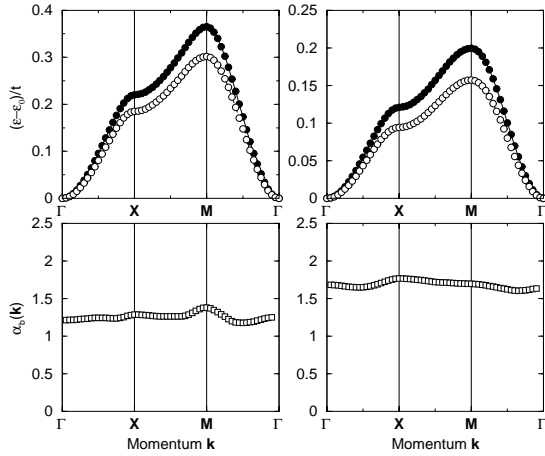


FIG. 2: Top panels: small Fröhlich polaron band dispersions along the main directions of the two-dimensional Brillouin zone. Left: $\lambda = 2.5$, right: $\lambda = 3.0$. Filled symbols is $\omega = 0.70 t$, open symbols is $\omega = 0.66 t$. Lower panels: the band structure isotope exponent for $\lambda = 2.5$ (left) and $\lambda = 3.0$ (right).

single-electron paths with all possible shifts satisfying the twisted boundary conditions with the weight $w(\mathbf{r}, \xi)$. The statistics for any number of \mathbf{k} points in the Brillouin zone are collected during a single QMC run [27].

The isotope exponent $\alpha_b(\mathbf{k})$ and DOS are presented in Figs. (1,2), and Fig.3, respectively, for the small Holstein polaron (SHP) with the short-range interaction, and for the small Fröhlich polaron (SFP) with the force given by Eq. (3). The polaron spectra are calculated for two phonon frequencies, $\omega = 0.70 t$ and $\omega = 0.66 t$, whose difference corresponds to a substitution of O¹⁶ by O¹⁸ in cuprates. There is a significant change in the dispersion law (topology) of SHP, Fig.1, which is less significant for SFP, Fig.2, rather than a simple band-narrowing (see also [26]). As a result, the isotope exponent

$$\alpha_b(\mathbf{k}) \approx 8 \frac{\epsilon_{\mathbf{k}}^{16} - \epsilon_{\mathbf{k}}^{18}}{\epsilon_{\mathbf{k}}^{16}}, \quad (6)$$

is \mathbf{k} -dependent, Fig.1 and Fig.2 (lower panels). The strongest dispersion of α_b is observed for SHP. Importantly, the isotope effect is suppressed near the band edge in contrast with the \mathbf{k} -independent strong-coupling isotope effect, Eq. (2). It is less dispersive for SFP, especially at larger λ , where the polaron energy band is well described by the strong-coupling Lang-Firsov expression.

Polaron DOS, $N(E) \equiv \sum_{\mathbf{k}} \delta(E - \epsilon_{\mathbf{k}})$, Fig.3, is less sensitive to topology, approximately scaling with the renormalised bandwidth. It reveals a giant isotope effect near the van Hove singularity because the bandwidth changes significantly with ω even in the intermediate-coupling regime.

The coherent motion of small polarons leads to metallic conduction at low temperatures. Our results, Figs.1-3,

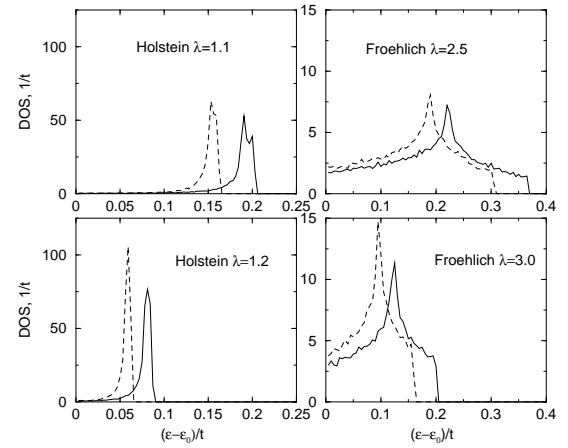


FIG. 3: Isotope effect on the polaron density of states. Solid line is $\omega = 0.70 t$, dashed line is $\omega = 0.66 t$.

show that there should be anomalous isotope effects on low-frequency kinetics and thermodynamics of polaronic conductors which depend on the position of the Fermi level in the polaron band. In fact, such effects have been observed in ferromagnetic oxides at low temperatures [9], and in cuprates [3, 4]. To address ARPES isotope exponents [8] one has to calculate the electron spectral function $A(\mathbf{k}, E)$ taking into account phonon side-bands (i.e. off diagonal transitions) along with the coherent polaron motion (diagonal transitions). Using the $1/\lambda$ expansion one obtains [12]

$$A(\mathbf{k}, E) = \sum_{l=0}^{\infty} \left[A_l^{(-)}(\mathbf{k}, E) + A_l^{(+)}(\mathbf{k}, E) \right], \quad (7)$$

where

$$A_l^{(-)}(\mathbf{k}, E) = \frac{Z [1 - n(E - l\omega)]}{(2N)^l l!} \times \sum_{\mathbf{q}_1, \dots, \mathbf{q}_l} \prod_{r=1}^l |\gamma(\mathbf{q}_r)|^2 \delta[E - l\omega - \zeta(\mathbf{k}_l^-)],$$

and

$$A_l^{(+)}(\mathbf{k}, \omega) = \frac{Z \cdot n(E + l\omega)}{(2N)^l l!} \sum_{\mathbf{q}_1, \dots, \mathbf{q}_l} \prod_{r=1}^l |\gamma(\mathbf{q}_r)|^2 \delta[E + l\omega - \zeta(\mathbf{k}_l^+)]. \quad (8)$$

Here $Z = \exp(-E_p/\omega)$, $\zeta(\mathbf{k}) = \epsilon_{\mathbf{k}} - \mu$, μ is the chemical potential, $n(E) = [\exp(\beta E) + 1]^{-1}$, $\mathbf{k}_l^{\pm} = \mathbf{k} \pm \sum_{r=1}^l \mathbf{q}_r$ and $\gamma(\mathbf{q})$ is the Fourier transform of the force $f(\mathbf{m}) = N^{-1} M^{1/2} \omega^{3/2} \sum_{\mathbf{q}} \gamma(\mathbf{q}) e^{i\mathbf{q} \cdot \mathbf{m}}$.

Clearly, Eq. (7) is in the form of a perturbative multi-phonon expansion. Each contribution $A_l^{(\pm)}(\mathbf{k}, E)$ to the spectral function describes the transition from the initial state \mathbf{k} of the polaron band to the final state \mathbf{k}_l^{\mp} with the emission (or absorption) of l phonons. Different from the conventional Migdal self-energy [5] the electron spectral function comprises two different parts in the

strong-coupling limit. The first ($l = 0$) \mathbf{k} -dependent term arises from the coherent polaron tunnelling, $A_{coh}(\mathbf{k}, E) = [A_0^{(-)}(\mathbf{k}, E) + A_0^{(+)}(\mathbf{k}, E)] = \pi Z \delta(E - \zeta_{\mathbf{k}})$ with a suppressed spectral weight $Z \ll 1$. The second *incoherent* part $A_{incoh}(\mathbf{k}, E)$ comprises all terms with $l \geq 1$. It describes excitations accompanied by emission and absorption of phonons. We note that its spectral density spreads over a wide energy range of about twice the polaron level shift E_p , which might be larger than the unrenormalised bandwidth $2zt$ in the rigid lattice. On the contrary, the coherent part shows a dispersion only in the energy window of the order of the polaron bandwidth. It is important that the *incoherent* background $A_{incoh}(\mathbf{k}, E)$ is dispersive (i.e. \mathbf{k} -dependent) for the long-range interaction. Only in the Holstein model with the short-range dispersionless e-ph interaction $\gamma(\mathbf{q}) = const$ the incoherent part has no dispersion.

Using Eq. (7) one readily predicts an isotope effect on the coherent part dispersion $\epsilon_{\mathbf{k}}$ and its spectral weight Z , and also on the incoherent background because Z , $\gamma(\mathbf{q})$, and ω all depend on M . While our prediction is qualitatively robust it is difficult to quantify the ARPES isotope effect in the intermediate region of parameters. The spectral function, Eq. (7), is applied in the strong-coupling limit $\lambda \gg 1$. While the main sum rule $\int_{-\infty}^{\infty} dE A(\mathbf{k}, E) = 1$ is satisfied, the higher-momentum integrals $\int_{-\infty}^{\infty} dE E^p A(\mathbf{k}, E)$ with $p > 0$, calculated with Eq. (7) differ from their exact values [28] by an amount proportional to $1/\lambda$. The difference is due to partial “un-

dressing” of high-energy excitations in the side-bands, which is beyond the lowest order $1/\lambda$ expansion. The role of electronic correlations should be also addressed in connection with ARPES. While the results shown in Figs. 1-3 describe band-structure isotope effects in slightly-doped conventional and Mott-Hubbard insulators with a few carriers, their spectral properties could be significantly modified by the polaron-polaron interactions [29], including the bipolaron formation [30] at finite doping. On the experimental side, separation of the coherent and incoherent parts in ARPES remains rather controversial [31].

In conclusion, we have calculated the isotope effect on the band structure of doped insulators employing a continuous-time quantum Monte-Carlo algorithm, and found its dispersion in the intermediate coupling regime which essentially depends on the radius and strength of the electron-phonon interaction. Using the strong-coupling electron spectral function we predicted an isotope effect on the weight and dispersion of the coherent part, and on the incoherent background. The exact isotope exponents, Fig. 1 and Fig. 2, could be instrumental in understanding of current and future experiments with isotope substituted oxides, and in assessing different analytical and semi-analytical approximations.

We would like to thank J. Devreese, J. Hirsch, A. Lanzara, J. Samson, and S. Trugman for illuminating discussions. ASA acknowledges support of this work by the Leverhulme Trust (London).

-
- [1] E. Maxwell, Phys. Rev. **78**, 477 (1950); C.A. Reynolds *et al.*, *ibid* 487 (1950).
[2] A.S. Alexandrov, Phys. Rev. B **46**, 14932 (1992).
[3] G. Zhao *et al.*, Nature **385**, 236 (1997).
[4] R. Khasanov *et al.*, Phys. Rev. Lett. **92**, 057602 (2004).
[5] A.B. Migdal, Zh. Eksp. Teor. Fiz. **34**, 1438 (1958) (Sov. Phys. JETP **7**, 996 (1958)).
[6] A. Lanzara *et al.*, Nature **412**, 510 (2001).
[7] X.J. Zhou *et al.*, cond-mat/0405130.
[8] G-H. Gweon *et al.*, APS Bulletin (March Meeting 2004), 158, to appear in Nature.
[9] A.S. Alexandrov, *et al.*, Phys. Rev. B **64**, 140404(R) (2001).
[10] S. Engelsberg and J.R. Schrieffer, Phys. Rev. **131**, 993 (1963).
[11] G.M. Eliashberg, Zh. Eksp. Teor. Fiz. **38**, 966 (1960) (Sov. Phys. JETP **11**, 696 (1960)).
[12] For a review see A.S. Alexandrov, *Theory of Superconductivity: from weak to strong coupling*, (IoP Publishing, Bristol-Philadelphia, 2003), pp. 95-158.
[13] S.A. Trugman *et al.*, Int. J. Mod. Phys. B **15**, 2707 (2001), and references therein.
[14] F. Marsiglio, Phys. Lett. A **180**, 280 (1993); A.S. Alexandrov, V.V. Kabanov, and D.K. Ray, Phys. Rev. B **49**, 9915 (1994); G. Wellein and H. Fehske, Phys. Rev. B **56** 4513 (1997), and references therein.
[15] J.E. Hirsch and E. Fradkin, Phys. Rev. **27**, 4302 (1983).
[16] H. De Raedt and A. Lagendijk, Phys. Rep. **127**, 233 (1985).
[17] A.S. Mishchenko *et al.*, Phys. Rev. Lett. **91** 236401 (2003).
[18] T. Holstein, Ann. Phys. **8**, 325, 343 (1959).
[19] J.H. Kim *et al.*, Phys. Rev. B **49**, 13065 (1994).
[20] A.S. Alexandrov, Phys. Rev. B **53**, 2863 (1996).
[21] A.S. Alexandrov and P.E. Kornilovitch, Phys. Rev. Lett. **82**, 807 (1999); *ibid*, J. Phys.: Condens. Matter **14**, 5337 (2002).
[22] H. Fehske, J. Loos, and G. Wellein, Phys. Rev. B **61**, 8016 (2000).
[23] J. Bonca and S.A. Trugman, Phys. Rev. B **64**, 094507 (2001).
[24] A.S. Alexandrov and A.M. Bratkovsky, Phys. Rev. Lett. **84**, 2043 (2000).
[25] I. G. Lang and Yu. A. Firsov, Zh. Eksp. Teor. Fiz. **43**, 1843 (1962) (Sov. Phys. JETP **16**, 1301 (1963)).
[26] P.E. Kornilovitch, Phys. Rev. Lett. **81**, 5382 (1998); *ibid*, Phys. Rev. B **60**, 3237 (1999).
[27] For more details see P. Spencer *et al.*, to be published.
[28] P.E. Kornilovitch, EuroPhys. Lett. **59**, 735 (2002).
[29] J. Tempere and J.T. Devreese, Phys. Rev. B **64**, 104504 (2001).
[30] A.S. Alexandrov and C.J. Dent, Phys. Rev. B **60**, 15414 (1999).
[31] A. Kaminski *et al.*, cond-mat/0311451.